Fast Intra- and Inter-Prediction Mode Decision in H.264 Advanced Video Coding

Mehdi Jafari
Islamic Azad University, S and R Branch
Department of Communication Engineering
P.O.Box 14515-775, Tehran, Iran
mjafari@mail.uk.ac.ir

Shohreh Kasaei
Sharif University of Technology
Department of Computer Engineering
P.O.Box 11365-9517, Tehran, Iran
skasaei@sharif.edu

Abstract

H.264/AVC, the latest video coding standard, achieves better video compression rates since it supports new features such as a large number of intra- and inter- prediction candidate modes. H.264/AVC adopts *rate-distortion optimization* (RDO) technique to obtain the best intra- and inter-prediction, while maximizing visual quality and minimizing the required bit rate. However, the RDO reduces the encoding speed via the exhaustive evaluation of all candidate modes. In this paper, in conjunction with an overview of proposed algorithms for fast intra-mode decision in H.264/AVC encoders, we decrease the encoding time by reducing the computational complexity of the cost function and the number of candidate modes. Also, a new algorithm based on the properties of similar predicted pixels and the feature of reference pixels is proposed. The proposed algorithms use spatial and transform domain features (such as edge information, simple directional properties of intra-mode, feature of reference pixels and adjacent blocks information in the intra- and inter-frame) to select a subset of all candidate modes. Subsequently, the RDO procedure uses the reduced subset of all candidate modes for extracting the final mode. Experimental results show that our algorithm, compared to the RDO and some other fast algorithms, reduces the total encoding time with negligible loss in PSNR and a slightly increased bitrate.

Keywords: H.264/AVC, Intra-prediction, RDO, similar predicted-pixels.

1. Introduction

As recent multimedia applications (using various types of networks) are growing rapidly, video compression requires higher performance as well as new features. The newest video coding standard is developed by the joint of video teams of ISO/IEC MPEG and ITU_T VCEG as the international standard 14496-10 (MPEG-4 part 10) *advanced video coding* (AVC) [1, 2]. H.264/AVC has gained more and more attention; mainly due to its high coding efficiency (the average bitrate saving up to 50% as compared to H.263+ and MPEG-4 Simple Profile), minor increase in decoder complexity compared to existing standards, adaptation to delay constraints (the low delay mode), error robustness, and network friendliness [1, 2]. Table 1 [3] and Figure 1 [4] show the performance comparisons using MPEG-2, MPEG-4 (ASP), and H.264/AVC. To achieve outstanding coding performance, H.264/AVC employs several powerful coding techniques such as 4x4 integer transform, inter-prediction with variable block-size motion compensation, motion vector of quarter-pel accuracy, in-loop deblocking filter, improved entropy coding such as *context-adaptive variable-length coding* (CAVLC) and *content-adaptive binary arithmetic coding* (CABAC), enhanced intra-prediction, multiple reference picture, and the forth. Due to this new features, encoder computational complexity is extremely increased compared to previous standards. This makes H.264/AVC difficult for applications with low computational capabilities (such as mobile devices). Thus until now, the reduction of its complexity is a challenging task in H.264/AVC.

Table 1: Average bit-rate reduction compared to prior coding schemes.

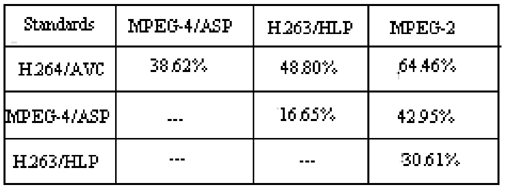

Standards	MPEG-4/ASP	H.263/HLP	MPEG-2
H.264/AVC	38.62%	48.80%	64.46%
MPEG-4/ASP	---	16.65%	42.95%
H.263/HLP	---	---	30.61%

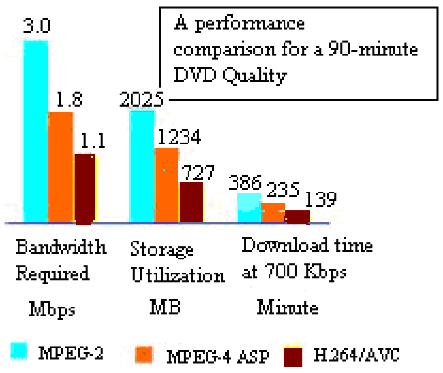

Figure1: Performance comparison of different video coding standards.

Among many new features, the intra-prediction technique is recognized to be one of the main factors that contribute to the success of H.264/AVC. H.264/AVC employs the Lagrangian RDO method to find out the best coding mode of intra-prediction with highest coding efficiency. Figure 2 [1] shows the RDO process. RDO technique requires a lot of computations since it tests the encoding process with all possible coding modes of intra-coding, and calculates their RD costs to choose the mode having the minimum cost. The intra-prediction mode decision is very complex and the number of computing RD cost values for luma and chroma of a macroblock is 592 [5]. Therefore, the computational burden of this type of brute force-searching algorithm is far more demanding than any existing video coding algorithm.

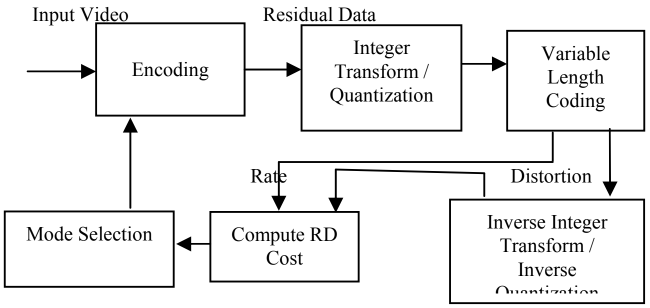

Figure 2: Computation of RD cost [1].

To reduce the computational complexity, many algorithms (such as fast motion estimation, fast inter-mode prediction, and fast intra-prediction) have been proposed. Fast mode selection for intra-prediction is considered in this paper; which is a challenging subject in H.264/AVC, since intra-prediction is a new topic in H.264/AVC coding with respect to other standards such as MPEG-1/2/4 and H.261/H.263 and so far no previous work exists for that. Fast intra-mode decision algorithms using edge detection histogram and local edge detection are proposed in [1, 6, 7]. However, their preprocessing stages still consume a coding time to detect the edge direction and to classify it into a limited direction. The performance of those methods is about 20~30% (or 55~65%) faster than the RDO method at the cost of 2% (or 5%) extra bits. There exist fast algorithms to select the optimal intra-prediction mode using simple directional masks in [8] with saving time of 70%, and statistical-based methods in [9] with saving time of 45%. Another fast intra-mode decision scheme is proposed in [10], where the encoding speed is approximately 30% faster than that of the RDO method. A new fast intra-prediction algorithm based on macroblock properties (FIPAMP) is presented in [11]. This algorithm can achieve 10% to 40% of computation reduction while maintaining similar PSNR and bit rate performance of H.264/AVC codes. In [12], an efficient intra-prediction (EIP) algorithm based on early termination, selective computation of highly probable modes, and partial computation of the cost function is presented. Also, an improved cost function to improve the coding performance is proposed in [13].

In [14], a fast algorithm based on the local edge information obtained by calculating edge feature parameters, and sub-sampling of matching operations is presented. That method can reduce the encoding time about 26% with less than 1.4% used extra bits and no more than 0.7 dB PSNR is sacrificed.

In this paper, we first present our new ideas to reduce the computational complexity of some previously proposed algorithms such as those presented in [1, 6, 7, 14, 19]. Then, we propose a method for fast intra-mode decision in which the number of 4x4 and 16x16 intra-mode for luma and 8x8 intra-mode for chroma has been reduced using directional edges and spatial correlation between current block and top-left blocks in I-frame. The proposed algorithm is based on the fact that for any intra-mode some pixels of a block are predicted with similar values such that the difference values between them for any mode must be zero. These similar pixels are along the existing edge in the block.

The cost for each intra-mode is extracted from the *sum of absolute differences* (SAD) of these similar pixels. Similar predicted pixels are extracted from JM7.1 (the JVT reference software [15]). After computing the simple costs the minimum and second minimum of cost are used as the two candidate modes. These candidate modes with adjacent blocks' information are used to decide about a subset of candidate modes for the final challenge. In the worst case, for intra-prediction of 4x4 luma and 16x16 luma only 3 and 2 modes, and for 8x8 chroma 2 modes are left for final mode decision made by RDO calculations. The proposed method consumes less encoding time by reducing the number of RDO computations and by reducing the time to obtain directional information. We have verified the proposed algorithm by implementing it on JM7.1 reference software and comparing it with the case of RDO search. Simulation results show the proposed method reduces the encoding time up to 47% with loss in PSNR and negligible increase of required bitrate. The remaining parts of the paper are organized as follows. We review the intra-prediction scheme of H.264/AVC and the mode selection method based on RDO technique in Sections 2 and 3, respectively. Section 4 presents the new and improved methods that are proposed for fast intra-mode decision methods. Simulation results are given in Section 5 and finally Section 6 concludes the paper.

2. Intra-Prediction in H.264/AVC

H.264/AVC defines a block-based hybrid video codec. It is mostly similar to the previous standards (H.261, H.263, MPEG-1, MPEG-2, and MPEG-4 Part 2-video). The elements common to all video coding standards that are presented in the current H.264/AVC recommendation are: an MB is 16x16 in size; luma is represented with higher resolution than chroma with 4:2:0 subsampling; motion compensation and block transforms are followed by scalar quantization and entropy coding, motion vectors are predicted from the median of the motion vectors of neighboring blocks, and so on. Some new functional elements such as intra-/inter-prediction, integer transformation, quantization, entropy coding are enhanced with some important changes that distinguish this standard from its predecessors. In common with earlier standards, H.264/AVC does not define the encoder, but defines the syntax of an encoded video bitstream together with the method of decoding the bitstream [16]. The codec combines intra-picture prediction with inter-picture prediction to exploit the spatial and temporal redundancy, respectively.

Intra-prediction is based on the observation that adjacent macroblocks tend to have similar properties. Therefore, as a first step in the encoding process for a given macroblock, one may predict the macroblock of interest from the surrounding macroblocks. The difference between the actual macroblock and its prediction is then coded; which results in fewer bits to represent the macroblock of interest.

Prediction may be formed for each 4x4 luma block (I4MB), 16x16 luma MB (I16MB), and 8x8 chroma block. The residual between the current MB and its prediction is then transformed, quantized, and entropy coded. For I4MB, which are selected in non-homogeneous area, there are 9 directional prediction modes, whereas for I16MB, which are selected in relatively homogeneous areas, there are 4 directional prediction modes. For 8x8 chroma blocks, there are 4 directional prediction modes, and the same mode is applied to two chrominance components (U and V). Chrominance is encoded in the same way as I16MB. For each macroblock, one prediction mode which defines partitioning of the macroblock is transmitted. For each mode and partition, one of several prediction directions is transmitted as well. In particular, for I16 only one direction for Luma is encoded, while it is necessary to transmit 16 directions for I4.

2.1 I4MB Prediction Modes

For prediction of 4x4 luminance blocks, the 9 directional modes consist of a DC prediction (Mode 2) and 8 directional modes; labeled 0, 1, 3, 4, 5, 6, 7, and 8 as shown in Figure 3(a). In Figure 3(b), the block (values of pixels "a" to "p") is to be predicted using A to Q. Note that pixels "A" to "Q" from neighboring blocks have already been encoded and may be used for prediction.

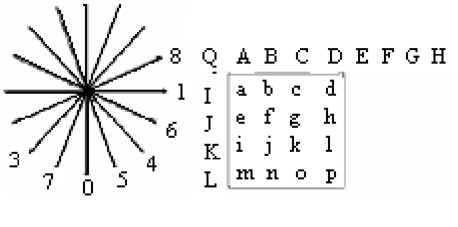

(a) (b)

Figure 3: (a) Intra-prediction modes for 4x4 luminance blocks. (b) Labeling of prediction samples.

Note that in some cases, not all of the samples "A-Q" are available within the current slice. In order to preserve independent decoding of slices, only samples within the current slice are available for prediction.

The DC prediction (mode 2), useful for those blocks with little or no local activities, is modified depending on which samples "A-M" are available; the other modes (1-8) may only be used if all of the required prediction samples are available (except that, if E, F, G, and H are not available, their value is copied from sample D). The arrows in Figure 5 indicate the direction of prediction in each mode. For modes 3-8, the predicted samples are formed from a weighted average of the prediction samples "A-Q". The encoder may select the prediction mode for each block that minimizes the residual between P and the block to be encoded.

Figure 4 shows a luminance macroblock in a QCIF formatted frame and a 4x4 luma block that is to be predicted. The samples above and to the left have previously been encoded and reconstructed and are therefore available in the encoder and decoder to form a prediction reference. The prediction block P is calculated based on the samples labeled "A-Q".

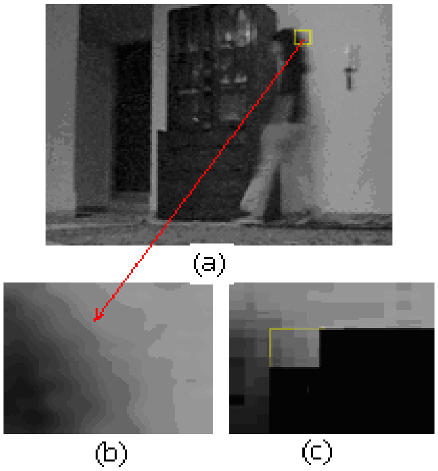

Figure 4: (a) 71st frame of original walking person sequence. (b) Original macroblock.
(c) 4x4 luma block to be predicted [16, 17].

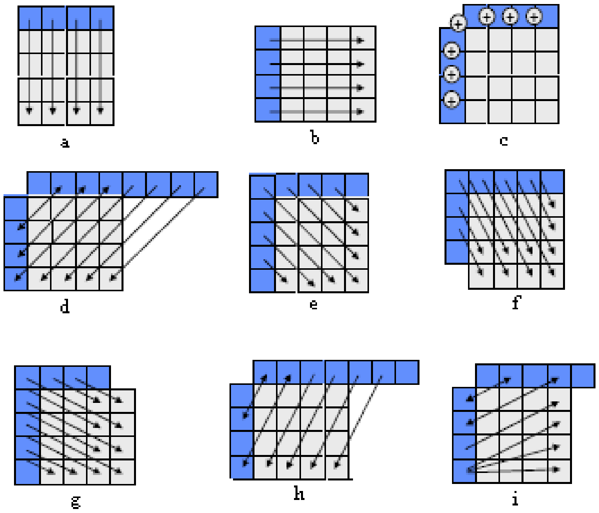

Figure 5: 4x4 luma prediction modes: (a) Mode 0 (vertical). (b) Mode 1 (horizontal). (c) Mode 2 (DC). (d) Mode 3 (diagonal down-left).
(e) Mode 4 (diagonal down-right), (f) Mode 5 (vertical-right). (g) Mode 6 (horizontal-down). (h) Mode 7 (vertical left). (i) Mode 8 (horizontal-up) [2].

The 9 prediction modes (0-8) are calculated for the 4x4 block shown in Figure 4. For example, in DC (mode 2) and diagonal down/right (mode 4) prediction, different samples are predicted by the algorithm illustrated in Figure 6.
Figure 7 shows the prediction block P created by each of the 9 predictions. The *sum of absolute error* (SAE) for each prediction indicates the magnitude of the prediction error.

```
 // Mode 0; make DC prediction
 s0 = 0;
 if (block_available_up && block_available_left)
 {
      s0 = (A+B+C+D+I+J+K+L+ 4)/(8);
 }
 else if (!block_available_up && block_available_left)
 {
   s0 = (I + J + K + L + 2)/4;
 }
 else if (block_available_up && !block_available_left)
 {
   // left edge
   s0 = (A + B + C + D + 2)/4;
 }
 else //if (!block_available_up && !block_available_left)
 {
   // top left corner, nothing to predict from
   s0 = 128;
 }

 for (j=0; j < 4; j++)
 {
   for (i=0; i < 4; i++)
   {
     // store DC prediction
     img->mprr[DC_PRED][i][j] = s0;
   }
 }
   // Mode DIAG_DOWN_RIGHT_PRED
 if   (block_available_up   &&   block_available_left   &&
block_available_up_left)
 {
   m = (L + 2*K + J + 2) / 4;
   i =n = (K + 2*J + I + 2) / 4;
   e =j =o = (J + 2*I + Q + 2) / 4;
   a=f=k=p= (I + 2*Q + A + 2) / 4;
   b=g=l = (Q + 2*A + B + 2) / 4;
   c=h= (A + 2*B + C + 2) / 4;
   d = (B + 2*C + D + 2) / 4;
}
```

Figure 6: A part of proposed intra-prediction algorithm in JM7.1 [15].

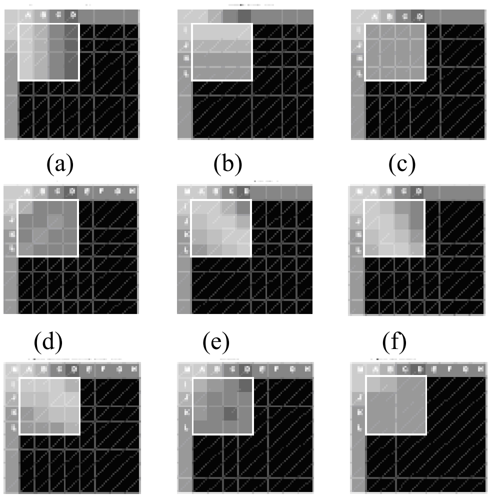
(a) (b) (c)

(d) (e) (f)

(g) (h) (i)

Figure 7: Prediction blocks (4x4): (a) Mode 0, SAE=325. (b) Mode 1, SAE=340. (c) Mode 2 (DC), SAE=342. (d) Mode 3, SAE=312. (e) Mode 4, SAE=352. (f) Mode 5, SAE=346. (g) Mode 6, SAE=347. (h) Mode 7, SAE=319. (i) Mode 8, SAE=358[18].

2.2 I16MB Prediction Modes

For regions with less spatial details *(i.e.,* flat regions), H.264/AVC supports 16x16 intra-coding; in which one of four prediction modes (DC, vertical, horizontal and planar) is chosen for the prediction of the entire luminance component of the macroblock as shown in Figure 8 [18], as:

- Mode 0 (vertical): extrapolation from upper samples (H).
- Mode 1 (horizontal): extrapolation from left-hand samples (V).
- Mode 2 (DC): mean of upper and left-hand samples (H+V).
- Mode 3 (Plane): a linear "plane" function is fitted to the upper and left-hand samples H and V (works well in areas with smoothly-varying luminance).

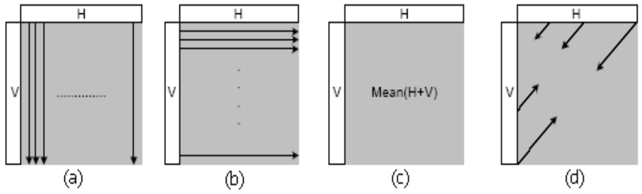

Figure 8: Intra 16x16 prediction modes: (a) Mode 0 (vertical). (b) Mode 1 (horizontal). (c) Mode 2 (DC). (d) Mode 3 (plane) [18].

Figure 9 shows a luminance macroblock with the previously-encoded samples at the upper and left-hand edges. The results of prediction (shown in Figure 10) indicate that the best match is given by mode 3. Intra 16x16 mode works best in homogeneous areas of an image.

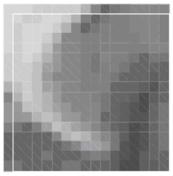

Figure 9: A 16x16 macroblock.

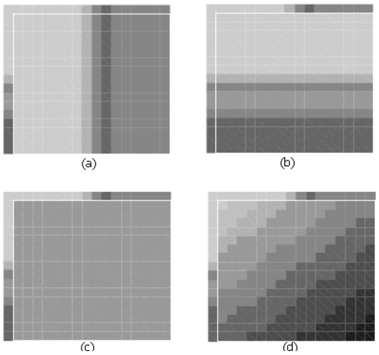

Figure 10: Intra 16x16 predictions: (a) Mode 0 (vertical), SAE=8990. (b) Mode 1 (horizontal), SAE=10898. (c) Mode 2 (DC), SAE=11210. (d) Mode 3 (plane), SAE=6264[18].

2.3 8x 8 Chroma Prediction Modes

H.264/AVC supports four chroma prediction modes for 8x8 chrominance blocks, similar to that of the I16MB prediction, except that the order of mode numbers is different: DC (Mode 0), horizontal (Mode 1), vertical (Mode 2), and plane (Mode 3). The same prediction mode is always applied to both chroma blocks. The chroma prediction is independent from luma prediction.

Finally, for I-frames, while all MBs are predicted as Intra, H.264/AVC encoder encodes the best mode using all mode combinations of luma and chroma and chooses the one that gives the best RDO performance. For P-frames, intra- and inter-prediction is done and RDO used for best prediction. Here, two sequences of QCIF and CIF formatted frames are encode using JM7.1. The results are shown for two I- and P-frame in Figures 11 and 12, respectively.

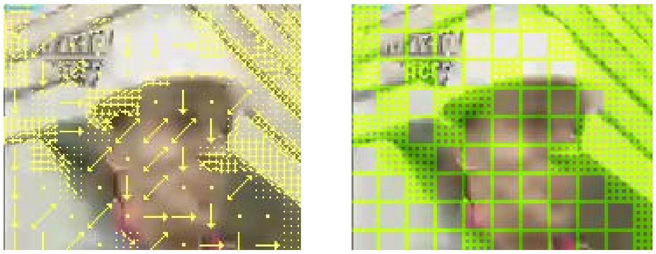

(a) (b)

Figure 11: I-frame of "*foreman"* sequence (QCIF). (a) I4MB and I16MB prediction mode decision. (b) I4MB and I16MB divisions.

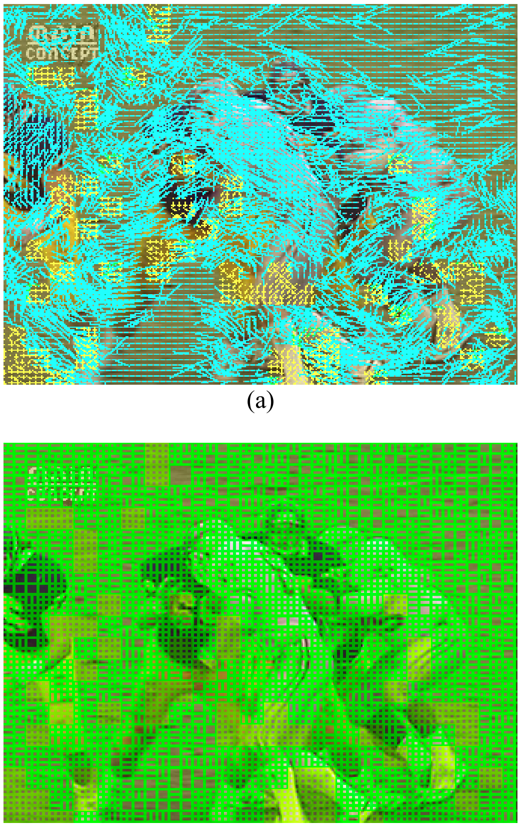

(a)

(b)

Figure 12: P-frame of "*football*" sequence (CIF). (a) I4MB and I16MB (yellow) and inter-prediction (blue) prediction mode decision. (b) I4MB, I16MB, and inter-mode divisions.

3. RDO Procedure

The RDO procedure to encode one MB in an I-frame is given below [5].

a) Search the best intra-mode for a 4x4 luma block among 9 modes that produces the minimum rate-distortion cost given by:

$$J\,(s,c,MODE\,|\,QP,\lambda_{\text{mode}}) = SSD(s,c,MODE\,|\,QP) + \quad \lambda_{MODE}R(s,c,MODE\,|\,QP) \tag{1}$$

Where QP is the macroblock quantization parameter, $\lambda = 0.85 \times 2^{(QP-12)/3}$ is the Lagrangian multiplier, and $MODE$ indicates one of the 9 prediction modes of a 4x4 luma block. *R (.)* represents the rate, *i.e.*, the number of bits associated with chosen *MODE*. *SSD (.)* denotes the *sum of the squared differences* between the original 4x4 block luminance signal denoted by *s* and its reconstructed signal denoted by *c*, computed as:

$$SSD(s,c,MODE\,|\,QP) = \sum_{x=1,\,y=1}^{4,4} (s(x,y) - c(x,y,MODE\,|\,QP)^2 \tag{2}$$

b) As contrary to the RDO technique for intra 4x4 luma block mode decision, determine the best intra-mode for a 16x16 macroblock among 4 modes by choosing the mode those results in the minimum s*um of absolute transformed difference* (SATD) given by:

$$SATD = \sum_{(x,y)\in b_k} |T\{I(x,y)-P(x,y)\}| \tag{3}$$

Where I and P represent the true and predicted pixel values, respectively, and T denotes the Hadamard transform.
c) Compare the RD cost for the two best modes, *i.e.*, the I4MB mode obtained from Step 1 and the I16MB mode obtained from Step 2, and choose the best one as the macroblock prediction mode.
d) Determine the best intra-mode for 8x8 chroma block among 4 modes, as I16, by minimizing Equation (1).

Also, in the H.264 JVT reference software JM7.3 [15], the *full search* (FS) algorithm is used to examine all the possible intra-prediction modes to find the best modes. The steps for best intra-mode are similar to RDO, but I16MB decision procedure (part (b)) can be summarized as:

1. Generate 4 prediction MBs according to 4 modes of I16MB and then calculate their residual MBs. For each residual MB:
2. Perform the Hadamard transform for each 4x4 block.
3. Extract all DCs from this sixteen 4x4 blocks and divide them by 4, to form another 4x4 block. Perform the Hadamard transform for this 4x4 block.
4. Sum up the absolute value of all Hadamard transform coefficients; use the summation as the cost. The best I16MB is the mode with the smallest cost.

For the FS algorithm, part (a) and (c) are similar to the RDO algorithm.

Also in a P-frame, intra- or inter-prediction can be selected. For intra-predictive modes the mentioned procedure is used. For inter-predictive modes, the motion estimation is done within a search range for the multiple reference frames. At last, the best prediction mode among all possible intra-/inter-predictive modes is achieved by minimizing Equ. (1), where *SSD* is defined as:

$$\begin{aligned} SSD(s,c,MODE|\,QP) = {} & \sum_{x=1,y=1}^{16,16}(s_y(x,y)-c_y(x,y,MODE|\,QP))^2 \\ & + \sum_{x=1,y=1}^{8,8}(S_u(x,y)-c_U(x,y,MODE|\,QP))^2 \\ & + \sum_{x=1,y=1}^{8,8}(S_v(x,y)-c_v(x,y,MODE|\,QP))^2 \end{aligned} \tag{4}$$

According to the RDO procedure of intra-prediction in H.264/AVC, the number of mode combinations for luma and chroma blocks in a macroblock is N_8x(16xN_4 + N_{16}), where N_8, N_4, and N_{16} , denote the number of modes for 8x8 chroma blocks, and 4x4 and 16x16 luma blocks, respectively [5]. In other words, for a macroblock to be intra-coded with the best mode in H.264/AVC, the RDO procedure will perform 592 rate-distortion computations for comparison. As a result, the complexity of the encoder is extremely high. To reduce the encoding complexity with little RD performance degradation, some fast intra-mode decision methods and new trends to improve them are proposed in the next sections.

4. Proposed Methods for Fast Intra-Prediction Mode Decision

This section presents some fast intra-prediction algorithms and our trends to improve them. Also, a new fast algorithm is presented that is based on similar predicted pixels. This is motivated by some observations in our experiments. The proposed method is based on several facts that we observed from the statistics of different sequences that:
a) For intra-prediction of luminance samples the probability of 4x4 block size is significantly higher than 16x16 block size at usual quantization parameters (20~35). This fact is shown for a wide variety of inputs using JM 7.1. Figure 13 shows the total number of 4x4 and 16x16 intra-coded macro blocks at different *quantization parameters* (QPs). Therefore fast detection of 4x4 intra-prediction mode can significantly improve the encoding speed at low QP, while 16x16 intra-prediction at large QPs.
b) The prediction modes of each block are correlated with those of neighboring 4x4 luminance blocks. The statistics generated using JM 7.1 encoder [15] shows that for a wide variety of inputs large neighboring blocks have the same I4 mode. There are four possible types of 4x4 blocks in a frame, based on their location in the frame (see Fig. 14).

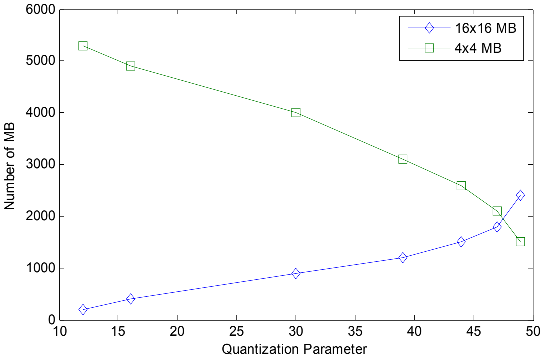

Figure 13: Number of 4x4 and 16x16 intra-coded macro blocks at different quantization parameters

The 4x4 blocks of category A for which neither top nor left block is present, of category B when left block is available but top block is not present, of category D when both top and left blocks are available. Among these, the 4x4 blocks of category D are significantly more in numbers and most of the computations are spent on deciding the appropriate mode for these blocks. From these observations, for each 4x4 D luma block, we obtain two candidate modes from adjacent blocks, *i.e.,* upper block and left block. For C category only left block and for B category only top block is considered as the candidate mode.

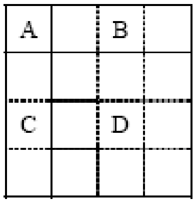

Figure 14: Types of 4x4 block based on availability of top and left 4x4 blocks[9].

c) Normally, pixels along the direction of local edge have similar values. Therefore, a good prediction can be achieved if we predict the pixels using those neighboring pixels that are in the same direction of the edge.
Generally, directional correlation of each block is consistent with directions of the edges. In [1], a fast intra-mode decision method is proposed, which is based on edge detection using the Sobel operation and edge direction histogram (EDH).
d) The residue values of intra-prediction are usually large compared to inter-prediction using *motion estimation* (ME) techniques.
e) The optimal mode (found by full search) and other “good” (second or third best) modes are most likely in similar directions.
f) The direction features of 4x4 blocks can be preserved roughly after down-sampling.
g) There are a total of 13 reference pixels for intra prediction of a 4x4 luma block, which locate at the up and the left of the 4x4 luma block. Experimental results show that the reference pixels of a 4x4 luma block are similar with each other with a high probability [22].

Based on these observations, we propose a fast intra-prediction mode selection algorithm. In this section some new ideas are combined with the fast mode selection algorithms introduced in [1, 6, 7, 14, 19] to improve their efficiency. Also, a new fast mode selection for I4MB and I16MB based on analyses of similar predicted pixels are proposed.

4.1 Improved Pan’s Method for Fast Decision of I4MB

Pan et al. in [1] present a fast mode selection for intra-prediction method in which the average edge direction of a given block is measured. The Sobel operators are first used to obtain directional vector of each pixel in a block by:

$$\vec{D}_{i,j} = \{dx_{i,j}, dy_{i,j}\} \qquad (5)$$

Where the Sobel operator are:

$$\begin{aligned} dx_{i,j} &= P_{i-1,j+1} + 2\times P_{i,j+1} + P_{i+1,j+1} - P_{i-1,j-1} - 2\times P_{i,j-1} - P_{i+1,j-1} \\ dy_{i,j} &= P_{i+1,j-1} + 2\times P_{i+1,j} + P_{i+1,j+1} - P_{i-1,j-1} - 2\times P_{i-1,j} - P_{i-1,j+1} \end{aligned} \qquad (6)$$

Where $dx_{i,j}$ and $dy_{i,j}$ represent the degree of difference in vertical and horizontal directions, respectively. Therefore, the amplitude and angle of each edge vector are calculated by:

$$Amp(\vec{D}_{i,j}) = | dx_{i,j} | + | dy_{i,j} | \tag{7}$$

and,

$$Ang(\vec{D}_{i,j}) = \frac{180^o}{\pi} \times \arctan(\frac{dy_{i,j}}{dx_{i,j}}) \ . \tag{8}$$

While *Ang* (.) is fitted into one of the following bins:

$$\begin{aligned} a_0 &= (-103.3^o, -76.6^o] \\ a_1 &= (-13.3^o, 13.3^o] \\ a_3 &= (35.8^o, 54.2^o] \\ a_4 &= (-54.2^o, -35.8^o] \\ a_5 &= (-76.6^o, -54.2^o] \\ a_6 &= (-35.8^o, -13.3^o] \\ a_7 &= (54.2^o, -76.7^o] \\ a_8 &= (13.3^o, 35.8^{o)} \end{aligned} \tag{9}$$

Then, the edge directional histogram of the block is analyzed as:

$$Histo(k) = \sum_{(m,n) \in set(k)} Amp(\vec{D}_{m,n}) \tag{10}$$

Where:

$$SET(k) \in \{i, j \mid Ang(\vec{D}_{m,n}) \in a_k)\} \tag{11}$$

Where k=0, 1, 3, 4, 8 refers to the 8 directional prediction modes.
The *edge direction histogram* (EDH) counts the number of pixels with similar edge directions. Therefore, the cell *k* with the maximum amplitude indicates that there is a strong edge along that direction that is used for making decision about the preferable direction mode. Figure 16 shows the edge direction histogram of Figure 15.

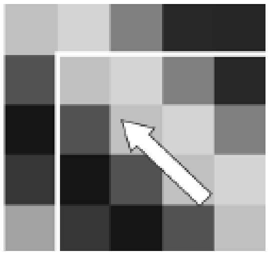

Figure 15: An example of 4x4 edge patterns and their proffered intra-prediction directions.

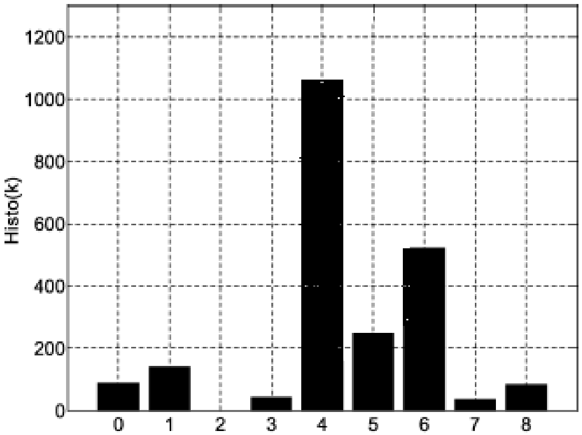

Figure 16: Edge direction histogram of Figure 15.

In Pan's method, for I4MB there are 4 modes (1 DC (mode 2), 1 from maximum amplitude of EDH and its 2 neighbors) while 2 modes (1 DC mode and 1 directional) for each 16x16 luma block and 8x8 chroma block. Here, we improve Pan's method. That is, eliminating the DC mode from the candidates if the direction of the block is obvious, and otherwise, choosing only DC mode. To check whether the DC of the block is clear or not, the *diff* value, given in Equation (12), is checked whether it is smaller than a threshold or not:

$$\begin{aligned} diff &= \sum_{i=0}^{i=15} | avg - p_i | \\ avg &= (\sum_{i=0}^{15} p_i + 8) >> 4 \end{aligned} \qquad (12)$$

The improved Pan's method is proposed as follows:

1. For edge directional histogram H, find its maximum. The corresponding mode is denoted by M1.
2. If *diff* > T, RDO procedure is carried out for 3 modes at the most (M1 and its two neighbors).
3. Else, if *diff* <T, RDO procedure I is carried out for two candidate modes at the most. DC with maximum of EDH (M1).
4. For I16MB, based on the same observation as above, after down-sampling by a factor of 2, if *diff1* > T1 only primary prediction mode decided by edge direction histogram is considered as a candidate for the best prediction mode. The *diff1* in this case is presented as:

$$\begin{aligned} diff1 &= \sum_{i=0}^{i=64} | avg - p_i | \\ avg &= (\sum_{i=0}^{64} p_i + 32) >> 6 \end{aligned} \qquad (13)$$

5. If *diff1* < T1, the maximum prediction mode and DC mode are chosen. The maximum prediction mode is extracted as I4MB but with DC and only 3 directions as:

$$\begin{aligned} a_0 &= [-112.5^o, -67.5^o) \\ a_1 &= [-22.5^o, 22.5^o) \\ a_3 &= [-67.5^o, -22.5^o) \end{aligned} \qquad (14)$$

where k=0, 1, and 3 refer to vertical, horizontal, and plane prediction modes, respectively.
6. For 8x8 chroma block, after down-sampling by a factor of 2, the same procedure as I16MB is used but by using Equ. (11).

Pan's method can reduce RDO calculation from 592 times to 132 times. Here, we improve Pan's method. The number of candidate modes and the RDO calculation in the worst and the best cases are shown in Table 2.

Table 2. Number of candidate modes.

Block Size	RDO	Pan's Method	Proposed Method (min)	Proposed Method (max)
4x4 (Y)	9	4	2	3
16x16 (Y)	4	2	1	2
8x8 (U/V)	4	3 or 2	1	2

Table 2 summarizes the number of candidates selected for RDO calculation based on edge direction histogram. As can be seen from Table 2, the encoder with the fast mode decision algorithm needs to perform only 33 or 100 RDO calculations, which are much less than that of Pan's method (132) and current H.264 video coding, RDO (592).

.

4.2 Fast Mode Selection for 4x4 Luma Block Using Subsampling and Edge Information

To extract the local edge information, the algorithm introduced in [14] divides a 4x4 block into four 2x2 blocks. Using A, B, C, and D to denote the sum of intensity of all pixels in the corresponding 2x2 blocks, given as:

$$\begin{aligned} A &= \sum_{i=0}^{1}\sum_{i=0}^{1} P_ij \qquad & B &= \sum_{j=2}^{3}\sum_{i=0}^{1} Pij \\ C &= \sum_{j=0}^{1}\sum_{i=2}^{3} Pij \qquad & D &= \sum_{j=2}^{3}\sum_{i=2}^{3} Pij \end{aligned} \qquad (15)$$

In order to obtain the local edge direction within a 4x4 block, this work introduces two edge feature parameters: vertical edge parameter F_v and horizontal edge parameter F_h as:

$$F_V = \left\lfloor \frac{(A+B)-(C+D)}{S} \right\rfloor$$
$$F_h = \left\lfloor \frac{(A+C)-(B+D)}{S} \right\rfloor \qquad (16)$$

Where S is a scaling factor [14]. According to these two parameters, the edge direction information within the current 4x4 block can be obtained. Table 3 shows the results.

On the other hand, the fast method only chooses the prediction mode along the edge as the *candidates of the best prediction modes* (CBPM). According to F_v and F_h, the determined different CBPMs for the current block corresponding to 7 cases (see Table 3) are obtained and summarized in Table 4.

Table 3: Edge direction information.

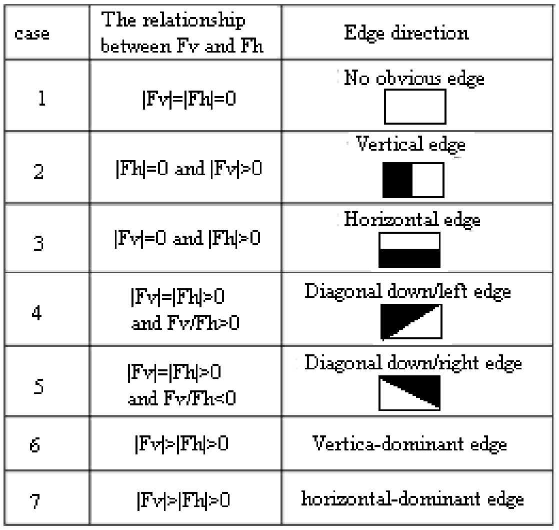

case	The relationship between Fv and Fh	Edge direction
1	|Fv|=|Fh|=0	No obvious edge
2	|Fh|=0 and |Fv|>0	Vertical edge
3	|Fv|=0 and |Fh|>0	Horizontal edge
4	|Fv|=|Fh|>0 and Fv/Fh>0	Diagonal down/left edge
5	|Fv|=|Fh|>0 and Fv/Fh<0	Diagonal down/right edge
6	|Fv|>|Fh|>0	Vertica-dominant edge
7	|Fv|>|Fh|>0	horizontal-dominant edge

Table 4: CBPMs according to F_v and F_h.

Case	1	2	3	4	5	6	7
CBPMs	2	0,2	1,2	3,2	4,2	0,5,7 3,4,2	1,6,8 3,4,2

Since the number of modes for case 6 and 7 are large and DC mode exists in all cases, we modify this method using improved Pan's method to extract the DC mode, so we choose DC if *diff*<T. Also, after detection of mode 6 and 7 from the above mentioned procedure we use Pan's method to detect the best method. From the simulation results, it can be seen that the proposed method has reduces the encoding time by 15.75% and 16.5% on average for "Container" and "Dancer" sequences, respectively. Also, simulated results shows that the proposed method has less than 1.1% used extra bits and no more than 0.2 dB PSNR is sacrificed. Also, we modified this algorithm for I16MB luma and 8x8 chroma in Subsection 4.4 to improve the proposed algorithm.

4.3 An Improved Feature-Based Method Using Fast Hadamard Transform

In [19], to address the feature selection problem, both spatial and frequency domain features are selected. Intuitively speaking, a good prediction should produce a small value of the *sum of absolute differences* SAD) and *sum of absolute transform difference* (SATD), which can be written as [20]:

$$SATD = \sum_{i=1}^{4}\sum_{j=1}^{4} \left| C_{ij} \right| \qquad (17)$$

Where C_{ij} denotes the element of *C* defined as:

$$C = T(I-P) \qquad (18)$$

where I and P denote the current block and its prediction, respectively, and T is a certain 2D orthonormal transform. In this work, for computational simplicity, T is chosen to be the separable Hadamard transform with 4-point along each dimension as:

$$T = \begin{bmatrix} 1 & 1 & 1 & 1 \\ 1 & 1 & -1 & -1 \\ 1 & -1 & -1 & 1 \\ 1 & -1 & 1 & -1 \end{bmatrix} \tag{19}$$

For a given 4 × 4 block, the SAD and SATD values can order according to their magnitudes, which is called the rank order. Most RDO modes fall in the window of 3 × 3 lowest ranks. Statistically, 93-95% of RDO modes are in such a window. Thus, it may search the RDO mode using the modes that fall in this window, which actually allows at most 3 distinctive Intra-prediction modes. Thus, we can narrow down the search range based on the joint feature of (*SAD, SATD*). It is worthwhile to point out that there always exist some candidate modes in the 3×3 window in all experiments performed. However, if there is no candidate mode in this window, we can enlarge the search window from 3 × 3 to 4 × 4 to find the possible candidate mode. The computation SATD can be improved using a fast Hadamard transform as below.

4.3.1 Fast Hadamard Transform Algorithm for SATD

The Hadamard transform defined in (19), without any fast algorithm, each mode needs 64 additions and totally 576 additions for all 9 modes. Now, we only need 212 additions and 39 shifts if we modified the fast algorithm presented in the [20]:
For example mode 0 is computed as:

$$P = \begin{bmatrix} a & b & c & d \\ a & b & c & d \\ a & b & c & d \\ a & b & c & d \end{bmatrix} \tag{20}$$

After computation of *TP,* all row vectors are zeros except the first row, is given as, [4a, 4b, 4c, 4d]. That we need only 4 shifts. Also the horizontal prediction gives:

$$P = \begin{bmatrix} a & a & a & a \\ b & b & b & b \\ c & c & c & c \\ d & d & d & d \end{bmatrix} \tag{21}$$

That the first row is nonzero as, [a+b+c+d, a+b-(c+d),a-b-(c+d),a-b+c-d)], That we need only 8 additions. Also other modes are as [20] and the final results is presented in table 5.

Table 5: Number of additions and shifts for the fast Hadamard transform.

Mode	Hadamard Transform	
	No. of ADDs	No. of Shifts
0	0	4
1	8	0
2	0	1
3	28	5
4	32	5
5	36	6
6	36	6
7	36	6
8	36	6
Total	212	39

Using this algorithm we can reduce the computational complexity of the main feature-based algorithm. We apply this fast transform to feature-based method. The simulation results show the reduction in encoding time, with approximately similar PSNR and bit rate.

4.4 Early Termination of RDO Calculation

Similar to Pan's method, for increasing the speed of the algorithm we use the early termination of RDO calculations for all proposed algorithms as in [1]. During the intra-coding of any prediction mode, the calculation can be terminated if it can foresee that the current mode will not be the best prediction mode. By early termination of the RDO calculations which is deemed to be suboptimal, a great timesaving can be achieved.

In the RDO, the coding cost consists of two parts: rate and distortion. After calculating the cost of rate, there might be cases that the cost of rate is higher than the coding cost of the best mode in the previous modes. This implies that the current mode will not be the best mode since its coding cost will not be the smallest. Therefore, in such cases we terminate the RDO calculation and hence the calculation of distortion will be eliminated.

An MB is encoded by either I4MB or I16MB predictions. In the RDO, the selection between these two coding modes is determined by the coding costs achieved by using each of these coding modes. After I16MB prediction coding, the I4MB prediction coding will apply to the sixteen 4x4 blocks in the MB and the cost of these blocks will be accumulated. However, if the accumulated cost before encoding the entire sixteen 4x4 blocks is already higher than that of I16MB prediction coding, the coding of the remaining of 4x4 blocks in the MB will be terminated prematurely.

4.5 Fast Mode Selection-Based on Similar Predicted Pixels

As an alternative method, we proposed a fast intra method using similar predicted pixels with combination of the presented algorithms in previous sections.

4.5.1 I4MB Fast Mode Decision

In Figure 17, the arrows show the direction of the desired mode and any two dots or squares, along that direction show the similar predicted pixels. The difference of this pixel can be used as a measure of direction prediction. We propose 9 simple masks to obtain DC and directional information within the block instead of using accurate edge detectors such as the Sobel operator. These masks are obtained by the formulas that are used for mode decision in JM 7.1. Some of formulas for mode decision are given in Figure 18 (a part of algorithm for intra-mode decision in JM 7.1). Using these masks, simple equations of 9 modes are yielded, as listed in Table 6. For final mode decision, the proposed algorithm uses the minimum and the second minimum cost shown in Table 6 as the two candidate modes that are consistent with their adjacent block information.

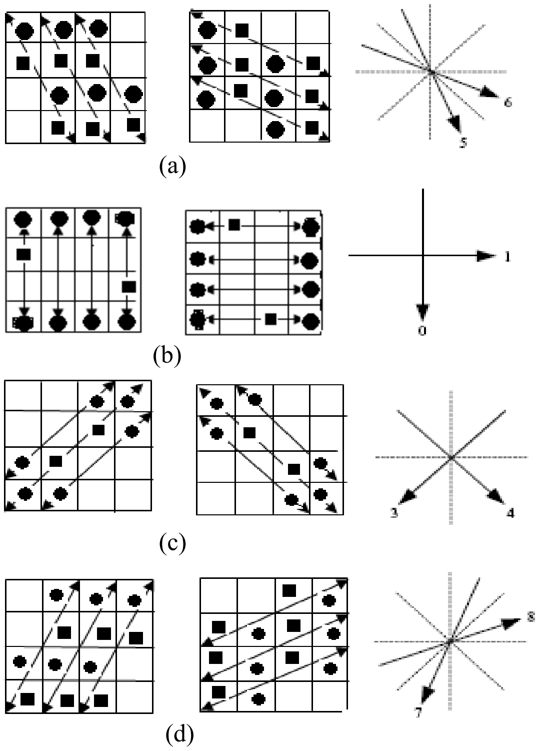

(a)

(b)

(c)

(d)

Figure 17. The proposed edge detector for 4x4 luma block. (a) Vertical right and horizontal down. (b) Vertical and horizontal. (c) Diagonal down left and diagonal down right. (d) Vertical left and horizontal up.

Based on these facts, Figure 19 shows the flowchart of the proposed algorithm. Steps of the proposed method are as follows:

1. Calculate the two most probable intra-prediction modes. These are the minimum (First Minumum Cost=MC1, mode MC1=M_MC1) and the second minimum (MC2, M_MC2) of costs evaluated by Table 6.

2. For 4x4 luma block, MAD (mean of absolute difference) of its reference pixels is computed, if it is smaller than a threshold, M_MC1 is selected. Go to step 10.

This result is yielded from this fact that if the similarity of reference pixels of a block is high, the difference between different prediction modes will be very small. For this case, it is not necessary to check all 9 prediction modes, but only one prediction mode is enough [22].

4. If MADH (mean of absolute difference of horizontal references) is less than a threshold and M_MC1 is a member of set {mode 0, mode 3, mode 7}, then M_MC1 is selected. Go to step 10.

5. Also, if MADV (mean of absolute difference of vertical references) is less than a threshold and M_MC1 is a member set of {mode 1, mode 8}, then M_MC1 is selected. Go to step 10.

It is obvious that if the similarity of horizontal reference pixels of a block is high, the difference between prediction results obtained with prediction modes 0, 3 and 7 will be very small. Also, if the similarity of vertical reference pixels of a block is high, the similarity between modes 1 and 8 is high.

Table 6 . Equations to select two candidate modes.

Mode	Mode Name	Cost Equation
0	Vertical	Cost= |a-m|+|b-n|+|c-o|+|d-p|+|e-m|+|d-l|
1	Horizontal	Cost= |a-d|+|e-h|+|i-l|+|m-p|+|b-d|+|m-o|
2	DC	Cost= |a-p|+|d-m|+|f-p|+|g-m|+|e-l|+|h-i|
3	Diag. Down/Left	Cost= |d-m|+|c-i|+|h-n|+|j-d|+|g-m|
4	Diag. Down/Right	Cost= |a-p|+|b-l|+|e-o|+|f-p|+|a-k|
5	Vertical Right	Cost= |a-j|+|e-n|+|b-k|+|f-o|+|c-l|+|g-p|
6	Horizontal Down	Cost= |a-g|+|b-h|+|e-k|+|f-l|+|i-o|+|j-p|
7	Vertical Left	Cost= |b-i|+|f-m|+|c-j|+|g-n|+|d-k|+|h-n|
8	Horizontal Up	Cost= |d-f|+|c-e|+|h-j|+|g-i|+|l-n|+|k-m|

6. If the modes for one of the top or the left blocks (M_A, M_B) are M_MC1, then Mode M_MC1 is chosen as the best candidate mode for the current block. Go to step 10.

7. If MC1-MC2 is less than a threshold, and MC1 and MC2 are adjacent, then MC is chosen. Go to step 10.

8. If MC1-MC2 is less than a threshold and MC1 and MC2 are not adjacent, the improved Pan's method is used. Go to step 10.

9. If MC1-MC2 is greater than a threshold, the Improved Pan's method is used.

10. Terminate.

As such, in the worst case only three different 4x4 intra-mode costs will be evaluated.

4.5.2 I16MB Based on Fast Hadamard Algorithm

As stated in FS algorithm, the decision for 16x16 block is based on SATD that is done on sixteen 4x4 subblocks. The computation of SATD can be achieved using fast algorithm presented in above section. This technique reduces the computational time efficiently.

4.5.3 I16MB Based on Similar Predicted Pixels (SPP)

The 16x16 block is down-sampled by a factor of 4 and the masks similar to the predicted pixels for 4x4 for horizontal, vertical, plane, and DC are used for making decision about the direction of the block.

4.5.4 I16MB based on Horizontal and Vertical Differences (HVD)

Let Δ_v and Δ_h denote the vertical and horizontal sum of differences between boundary pixels of current block and its adjacent block, respectively [8]:

$$\Delta_v = \sum_{i=0}^{15} \left| u_i - cu_i \right|, \qquad \Delta_h = \sum_{i=0}^{15} \left| l_i - cl_i \right| \tag{21}$$

where:

u_i : *boundary pixels of upper MB*
cu_i : *upper boundary pixels of current MB*
l_i : *boundary pixels of left MB*
cl_i : *left boundary pixels of current MB*

This method obtains candidate modes by using two differences values, under the conditions as follows:
1- $\Delta_v - \Delta_h$>T candidate modes are DC mode and horizontal mode.
2- $\Delta_h - \Delta_v$>T candidate modes are DC and vertical mode.
3- $|\Delta_v - \Delta_h|$ <T candidate modes are DC mode and plane mode.
4- Finally, determine the best mode among candidate modes by choosing the mode that results in the minimum SATD. For reducing the encoding time we can use the fast Hadamard procedure for SATD computation.

```
//make DC prediction:

a~p=(A+B+C+D+I+J+K+L+4)>> (BLOCK_SHIFT + 1);

// Mode DIAG_DOWN_LEFT_PRED

  a = (A + C + 2*(B) + 2) >> 2;
  b =e= = (B + D + 2*(C) + 2) >> 2;
  c =f=i== (C + E + 2*(D) + 2) >> 2;
  d=g=j=m= (D + F + 2*(E) + 2) >> 2;
  h=k=n= (P_E + P_G + 2*(P_F) + 2) >> 2;
  l=o= (F + H + 2*(G) + 2) >> 2;
  p = (G + 3*(H) + 2) >> 2;

// Mode VERT_LEFT_PRED

  a = (A + B + 1) >> 1;
  b =i=  (B + C + 1) >> 1;
  c = j = (C + D + 1) >> 1;
  d = k = (D + E + 1) >> 1;
  l = (E + F + 1) >> 1;
  e = (A + 2*B + C + 2) >> 2;
  f=m= (B + 2*C + D + 2) >> 2;
  g=n = (C + 2*D + E + 2) >> 2;
  h=o = (D + 2*E + F + 2) >> 2;
  p = (E + 2*F + G + 2) >> 2;

  // Mode DIAG_DOWN_RIGHT_PRED

 m = (L + 2*K + J + 2) >> 2;
 i =n = (K + 2*J + I + 2) >> 2;
```

Figure 18: Algorithm for some directional mode in JM 7.1

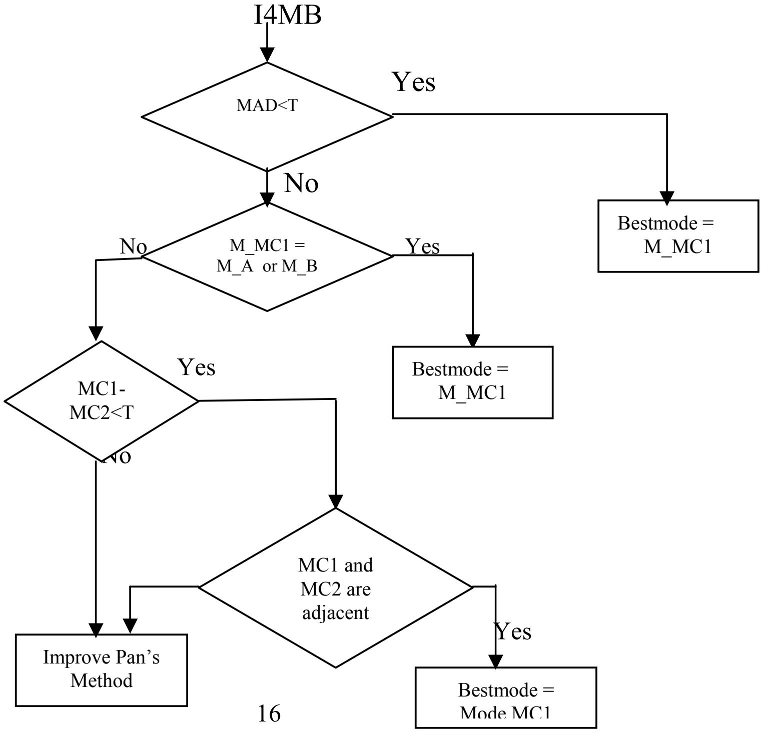

Figure 19. Flowchart for proposed fast intra-mode decision of 4x4 luminance blocks with low quantization.

4.5.5 Fast Mode Selection for 8x8 Chroma Block

For 8x8 chroma blocks, we apply a similar method to the method used for 16x16 luma macroblock (parts 4.5.3 and 4.5.4) except that we also apply a down-sampling by a factor of 2. Also, similar predicted pixel is used for 8x8 chroma blocks, after sub-sampling by a factor of 2.

5. Experimental Results

Our proposed algorithm was implemented into JM7.1, provided by JVT according to the test conditions specified in VCEG-N81 document as listed in Table 7[21]. Simulations were carried out on the recommended sequences with various quantization parameters for IPPP… type and I-frame only type. For IPPP… experiments, the total number of frames is 300 for each sequence, and the period of I-frame is 100. The used test platform is Pentium IV-2.8 GHz with 256 Mbytes RAM.

Table 7: Experiment condition.

GOP	IIIII or IPPP
Codec	JM 7.1
MV search range	±16
QP	10, 16, 24,28,36,40
Number of Reference	1
Common coding option	Hadamard transform, CABAC, RDO is enabled
Size	CIF and QCIF
Number of Frames	300

Comparisons with the case of exhaustive search (RDO) were performed with respect to the change of average PSNR (ΔPSNR), the change of average data bits (ΔBit), and the change of average encoding time (ΔTime), respectively.
The PSNR is derived from average PSNRs of luma component (Y) and chroma component (U, V) based on below equations:

$$\overline{PSNR} = 10 \log_{10}\left(255^2 \big/ \overline{MSE} \right) \tag{22}$$

where,

$$\overline{MSE} = \frac{4 \times MSE_Y + MSE_U + MSE_V}{6} \tag{23}$$

with

$$MSE_Y = \frac{65025}{10^{\frac{PSNR_Y}{10}}} \tag{24}$$

$$MSE_U = \frac{65025}{10^{\frac{PSNR_U}{10}}} \tag{25}$$

$$MSE_V = \frac{65025}{10^{\frac{PSNR_V}{10}}} \tag{26}$$

Therefore, in the rest of this paper we use the overall PSNR value of all the three components Y, U and V using Equation (22).

Also, in order to evaluate the time saving of the proposed fast intra-mode decision algorithm, the following calculation is defined to find the time differences. Let T_{ref} denote the coding time used by JM7.1 encoder and T_{prop} be the time taken by the faster intra-prediction algorithm, and $\Delta\ time$ be defined as:

$$\Delta\, Time\ \ \% = \frac{T_{prop} - T_{ref}}{T_{ref}} \times 100 \tag{27}$$

Also, bitrate increase is defined as:

$$\Delta Bitrate\ \% = \frac{bitrate_{prop} - bitrate_{ref}}{bitrate_{ref}} \times 100 \tag{28}$$

A group of experiments were carried out on different sequences and the results are shown below. The experiments were ordered in 8 states as listed in Table 8. The encoding bit rates, the PSNR values, and the time saving factor (as compared with the H.264 RDO method) for 4 test sequences with different quantization parameters are shown in Tables 9~14. Also, Tables 9~11 and 12~14 show the experimental results for IPPPP and IIII sequences, respectively. These tables compare the rate, distortion, and complexity of proposed algorithms with RDO procedure. Generally speaking, as can be seen from this tables, we have saved 47~58% of the total encoding time at the expense of only 0.1~1.5% rate increase in average and 0.015 distortion loss in average for these test sequences.

Figures 20, 21, and 22 show the examples of RD and the complexity curves of sequences "*Akiyo*" (class A), "*Foreman*" (Class B), and "*Stefan*" (Class C) for IPPP sequences. From these figures, one can see that the proposed fast intra-mode decision scheme gives almost identical RD performance while providing a speed-up factor (ratio of encoding time using the RDO technique and the proposed scheme) of 3-6. In this figure the RDO, improved Pan's method, improved feature-based and 3 forms of fast proposed methods are compared (see Table 8). We see that for proposed algorithms the rate-distortion performance loss increases slightly with a high complexity reduction. **For subjective quality comparison purposes, the reconstructed frames based on RDO and the proposed methods are captured at QP of 22 are shown in Figure 23 and 24 for *Foreman* and *New* sequences, respectively.**

Table 8. Different methods of experiment.

Category	I4MB	I16MB, Chroma	Early Terminatio n
RDO	RDO	RDO	NO
M1	Pan's Method	RDO	Yes
M2	Feature-Based Method	RDO	Yes
M3	Alg. 4.1	RDO	Yes
M4	Alg. 4.3	RDO	Yes
M5	Alg. 4.5.1	RDO	Yes
M6	Alg. 4.5.1	Alg. 4.5.3	Yes
M7	Alg.4.5.1	Alg. 4.5.4	Yes

6. Conclusion

In this paper, in conjunction with an overview of previous proposed algorithms based on EDH, Joint features of SAD/SATD, and statistical properties of natural video sequences for fast intra-mode decision in the H.264/AVC encoders, we decreased the encoding time by reducing the computational complexity of the cost function and the number of candidate modes. Experimental results of proposed algorithms show that the number of mode combinations for luma and chroma blocks in an MB that takes part in RDO calculation process has been reduced significantly with respect to original algorithms with negligible reduction in PSNR and negligible increase of bitrate.

At last, in order to achieve a better performance of computational complexity some new ideas with some strength point of improved algorithms are combined, and a new algorithm is presented**.** The simulation results show that the proposed algorithm reduces the number of RDO calculations with respect to original and improved algorithms with negligible loss in PSNR and negligible bitrate increase. The proposed algorithm can be used for challenging work of intra-prediction mode decision in the H.264/AVC video encoders with low computational cost

Table 9. Simulation results for IPPP type sequences.
Distortion comparison.

		Δ *PSNR* (*dB*)				
		10	16	22	32	40
Foreman	M1	-0.081	-0.079	-0.077	-0.065	-0.061
	M2	-0.5	-0.2	-0.1	0.0	0.1
	M3	-0.09	-0.081	-0.073	-0.05	-0.05
	M4	-0.30	-0.27	-0.012	-0.015	-0.01
	M5	-0.012	-0.01	-0.012	-.002	-.001
	M6	-0.3	-0.17	-0.125	-0.014	-0.02
	M7	-0.1	-0.014	-0.057	-0.018	-0.130
News	M1	-0.073	-0.071	-0.067	-0.064	-0.062
	M2	-0.047	-0.023	-0.01	0.00	0.0
	M3	-0.061	-0.060	-0.059	-0.50	-0.001
	M4	-0.03	-0.01	-0.00	-0.01	0.01
	M5	-0.020	-0.13	-0.016	-0.013	-0.120
	M6	-0.017	-0.008	-0.010	-0.015	0.00
	M7	-0.001	-0.007	-0.003	-0.014	-0.010
Container	M1	-0.089	-0.083	-0.081	-0.076	-0.074
	M2	-0.51	-0.17	-0.1	-0.1	0.00
	M3	-0.080	-0.065	-0.067	-0.069	-0.032
	M4	-0.46	-0.21	-0.01	-0.02	-0.03
	M5	-0.10	-0.204	-0.013	-0.013	-0.032
	M6	-0.120	-0.340	-0.036	-0.01	-0.001
	M7	-0.301	-0.010	-0.014	-0.012	-0.040
Silent	M1	-0.032	-0.035	-0.033	-0.032	-0.029
	M2	-0.04	-0.037	-0.023	-0.019	-0.01
	M3	-0.1	-0.02	-0.01	-0.02	0.00
	M4	-0.03	-0.01	-0.23	-0.012	-0.013
	M5	-0.324	-0.014	-0.080	-0.001	-0.035
	M6	-0.610	-0.317	-0.014	-0.012	-0.023
	M7	-0.230	-0.132	-0.013	-0.012	-0.017

Table 10: Simulation results for IPPP type sequences.
Rate comparison.

		Δ *Bit* %				
		10	16	22	32	40
Foreman	M1	1.650	1.540	1.536	1.354	1.230
	M2	1.050	1.004	0.962	0.987	0.870
	M3	1.230	1.210	1.035	0.670	0.345
	M4	1.032	0.890	0.634	0.425	0.478
	M5	1.130	0.735	0.917	0.890	0.098
	M6	1.325	1.230	0.725	0.675	0.0346
	M7	2.010	0.980	0.930	0.427	0.092
News	M1	1.534	1.001	1.022	1.030	0.924
	M2	0.924	0.940	0.876	0.830	0.910
	M3	1.021	0.932	0.982	0.760	0.567
	M4	1.120	0.0942	0.876	0.320	0.314
	M5	1.098	0.954	0.897	0.830	0.210
	M6	2.010	0.0845	0.872	0.828	0.621
	M7	2.120	0.932	0.489	0.762	0.412
Container	M1	1.803	1.902	1.090	0.950	0.921
	M2	0.983	0.987	0.732	0.510	0.321
	M3	1.673	0.982	0.879	0.340	0.450
	M4	1.345	0.941	0.512	0.710	0.342
	M5	2.340	0.980	0.987	0.604	0.324
	M6	1.348	0.821	0.742	0.812	0.436
	M7	2.100	0.932	0.980	0.434	0.431
Silent	M1	0.923	0.987	0.875	0.875	0.745
	M2	1.624	0.720	0.945	0.742	0.439
	M3	2.100	0.789	0.870	0.615	0.370
	M4	2.301	0.872	0.425	0.576	0.346
	M5	1.250	0.99	0.612	0.512	0.367
	M6	2.001	0.832	0.874	0.540	0.213
	M7	2.010	1.09	0.982	0.435	0.912

Table 11. Simulation results for IPPP type sequences.
Complexity comparison.

		Δ *Time* %				
		10	16	22	32	40
Forman	M1	-37.05	-35.42	-33.49	-32.60	-30.45
	M2	-35.23	-37.34	-43.24	-44.25	-45.5
	M3	-42.23	-39.25	-35.24	-35.02	-35.25
	M4	-39.95	-41.32	-41.23	-43.47	-44.32
	M5	-43.50	-42.23	-42.12	-40.25	-38.25
	M6	-48.31	-47.6	-45.25	-42.25	-42.12
	M7	-49.21	-43.32	-44.23	-47.25	-48.10
News	M1	-41.32	-38.24	-35.24	-31.12	-31.10
	M2	-38.45	-39.25	-40.25	-42.13	-43.23
	M3	-43.25	-41.50	-40.21	-39.34	-38.22
	M4	-41.25	-42.02	-43.02	-43.24	-44.23
	M5	-40.24	-40.34	-39.49	-39.56	-38.97
	M6	-43.23	-42.34	-40.31	-40.12	-39.56
	M7	-49.25	-48.27	-47.34	-47.12	-43.4
Container	M1	-31.03	-35.26	-34.02	-33.03	-34.25
	M2	-33.24	-34.25	-37.22	-39.44	-36.25
	M3	-33.24	-34.25	-37.22	-39.44	-36.25
	M4	-37.88	-39.50	-41.56	-43.23	-44.41
	M5	-41.25	-40.45	-40.37	-39.33	-38.01
	M6	-41.50	-40.23	-40.12	-39.13	-37.50
	M7	-45.50	-47.34	-46.34	-44.20	-40.35
Silent	M1	-36.02	-35.01	-31.02	-30.98	-30.37
	M2	-35.46	-37.89	-37.33	-39.42	-41.32
	M3	-40.21	-39.25	-39.10	-38.23	-38.12
	M4	-37.30	-38.50	-39.23	-41.78	-42.73
	M5	-41.34	-39.55	-39.33	-39.10	-38.28
	M6	-42.20	-41.47	-40.38	-39.59	-38.20
	M7	-45.46	-43.99	-43.22	-42.67	-39.78

Table 12. Simulation results for IIII type sequences. Distortion comparison.

		Δ *PSNR*				
		10	16	22	32	40
Forman	M1	-0.060	-0.065	-0.064	-0.063	-0.051
	M2	-0.45	-0.021	-0.01	0.001	0.10
	M3	-0.08	-0.070	-0.062	-0.05	-0.05
	M4	-0.130	-0.122	-0.022	-0.010	-0.01
	M5	-0.020	-0.011	-0.021	-.001	-.011
	M6	-0.13	-0.017	-0.120	-0.020	-0.012
	M7	-0.11	-0.020	-0.030	-0.020	-0.013
News	M1	-0.052	-0.060	-0.042	-0.050	-0.051
	M2	-0.037	-0.030	-0.010	0.010	-0.01
	M3	-0.050	-0.051	-0.042	-0.140	-0.010
	M4	-0.022	-0.02	-0.10	-0.02	0.010
	M5	-0.032	-0.020	-0.024	-0.022	-0.024
	M6	-0.023	-0.019	-0.025	-0.027	0.010
	M7	-0.012	-0.015	-0.012	-0.025	-0.022
Container	M1	-0.059	-0.064	-0.062	-0.056	-0.068
	M2	-0.052	-0.054	-0.201	-0.012	0.001
	M3	-0.182	-0.045	-0.053	-0.048	-0.042
	M4	-0.056	-0.031	-0.042	-0.032	-0.013
	M5	-0.120	-0.323	-0.033	-0.054	-0.067
	M6	-0.230	-0.030	-0.051	-0.042	-0.023
	M7	-0.410	-0.110	-0.124	-0.032	-0.062
Silent	M1	-0.061	-0.054	-0.053	-0.041	-0.035
	M2	-0.050	-0.043	-0.030	-0.023	-0.014
	M3	-0.051	-0.034	-0.042	-0.032	0.020
	M4	-0.043	-0.051	-0.024	-0.064	-0.072
	M5	-0.092	-0.037	-0.056	-0.037	-0.042
	M6	-0.271	-0.302	-0.045	-0.052	-0.041
	M7	-0.260	-0.182	-0.049	-0.053	-0.046

Table 13. Simulation results for IIII type sequences.
Rate comparison.

		Δ *Bits* %				
		10	16	22	32	40
Forman	M1	1.320	1.340	1.572	1.142	1.370
	M2	1.321	1.234	0.985	0.997	0.980
	M3	1.310	1.410	1.244	0.887	0.547
	M4	1.142	0.993	0.719	0.562	0.539
	M5	1.142	0.852	1.017	1.090	0.198
	M6	1.241	1.322	0.834	0.752	0.142
	M7	1.910	1.080	0.934	0.526	0.192
News	M1	1.132	1.201	1.132	1.215	0.956
	M2	0.970	0.967	0.893	0.742	0.932
	M3	1.130	1.334	0.923	0.950	0.822
	M4	1.120	0.0942	0.876	0.320	0.314
	M5	1.180	1.095	0.985	0.713	0.515
	M6	1.350	0.275	0.980	0.690	0.982
	M7	1.320	0.978	0.999	0.957	0.689
Container	M1	1.203	1.002	1.042	1.095	0.942
	M2	1.310	1.124	1.231	0.981	0.739
	M3	1.312	0.990	0.989	0.720	0.730
	M4	1.345	0.941	0.512	0.710	0.342
	M5	2.127	0.999	1.087	0.824	0.612
	M6	1.101	0.981	0.802	0.922	0.812
	M7	1.900	0.912	1.210	0.814	0.011
Silent	M1	1.223	1.087	0.921	0.905	0.980
	M2	1.750	0.930	1.012	0.590	0.610
	M3	1.940	0.312	0.590	0.435	0.560
	M4	1.920	0.702	0.215	0.736	0.416
	M5	1.467	0.929	0.732	0.702	0.621
	M6	1.209	0.212	0.744	0.503	0.021
	M7	1.910	1.100	0.907	0.515	0.435

Table 14. Simulation results for IIII type sequences.

Complexity comparison.

		Δ *Time* %				
		10	16	22	32	40
Forman	M1	-47.15	-46.12	-43.29	-49.10	-47.25
	M2	-50.13	-47.10	-52.45.	-54.20	-55.50
	M3	-55.34	-59.25	-45.34	-42.82	-45.15
	M4	-50.05	-51.32	-52.30	-51.27	-54.12
	M5	-53.21	-55.13	-54.34	-52.31	-54.16
	M6	-55.21	-57.30	-54.12	-51.05	-52.10
	M7	-58.10	-51.20	-53.37	-55.85	-57.21
News	M1	-52.24	-58.20	-53.61	-51.90	-50.46
	M2	-49.50	-52.50	-50.15	-52.42	-51.02
	M3	-50.12	-51.23	-50.78	-49.74	-48.89
	M4	-51.34	-52.43	-53.19	-52.10	-52.13
	M5	-51.35	-50.27	-49.91	-50.06	-49.55
	M6	-51.30	-52.04	-51.21	-51.62	-49.96
	M7	-58.45	-56.31	-57.03	-52.53	-50.04
Container	M1	-46.23	-45.32	-44.72	-43.67	-44.39
	M2	-46.42	-48.53	-47.43	-49.64	-46.42
	M3	-45.34	-44.65	-47.39	-49.51	-48.12
	M4	-47.90	-50.20	-51.06	-52.43	-54.10
	M5	-51.85	-50.75	-52.37	-56.12	-48.32
	M6	-52.60	-50.43	-52.32	-56.43	-47.34
	M7	-55.40	-57.64	-56.04	-55.12	-52.30
Silent	M1	-49.21	-46.31	-43.32	-45.38	-43.29
	M2	-49.76	-49.90	-50.03	-49.62	-51.12
	M3	-50.30	-49.50	-50.37	-49.38	-48.92
	M4	-51.22	-58.60	-51.73	-53.38	-54.13
	M5	-50.49	-53.18	-58.28	-59.43	-58.71
	M6	-52.12	-51.31	-50.16	-49.18	-50.23
	M7	-55.16	-50.19	-50.22	-52.67	-56.82

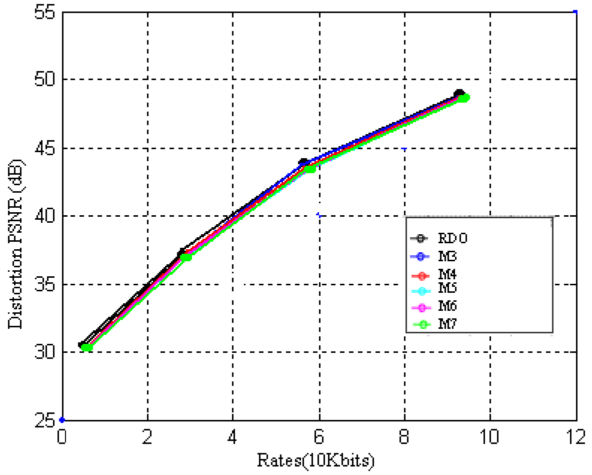

(a)

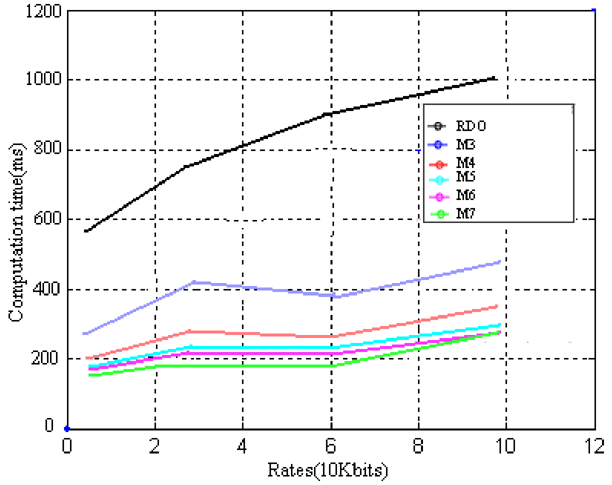

(b)

Figure 20: Akiyo sequence, (IPPP seq.). (a) R-D performance, (b) computational complexity.

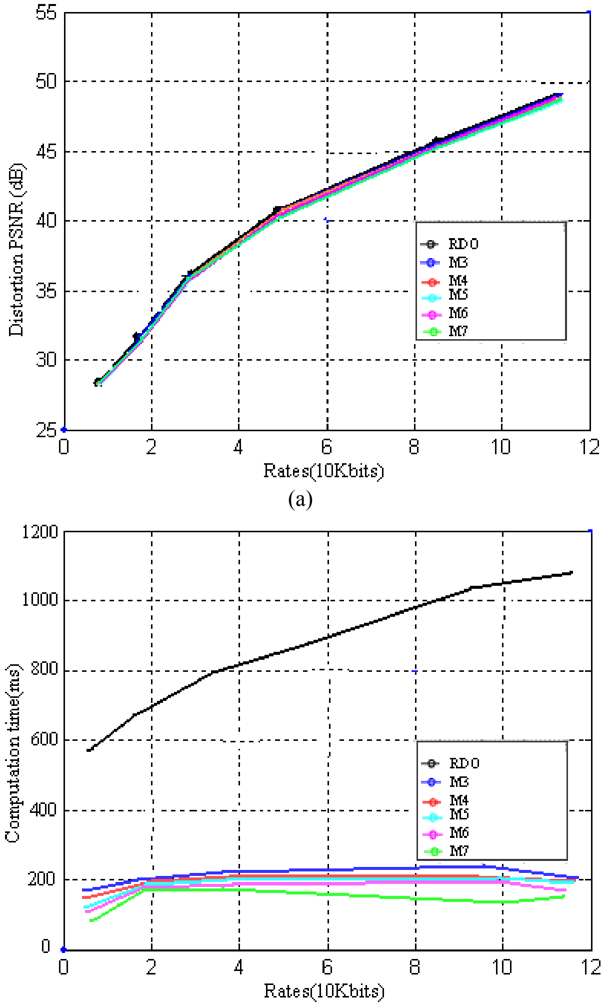

(a)

(b)

Figure 21: Foreman sequence, (IPPP seq.). (a) R-D performance, (b) computational complexity

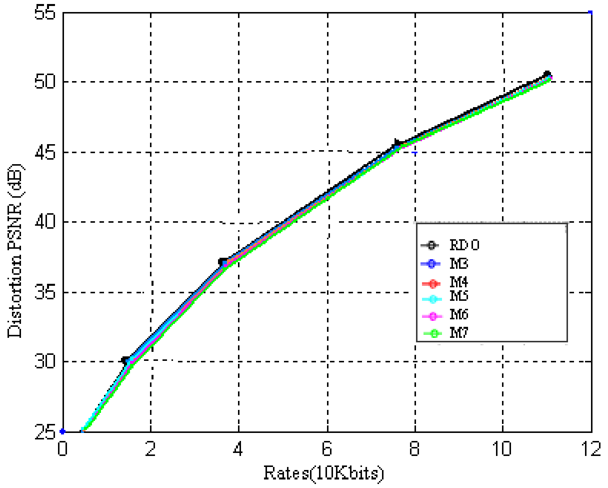

(a)

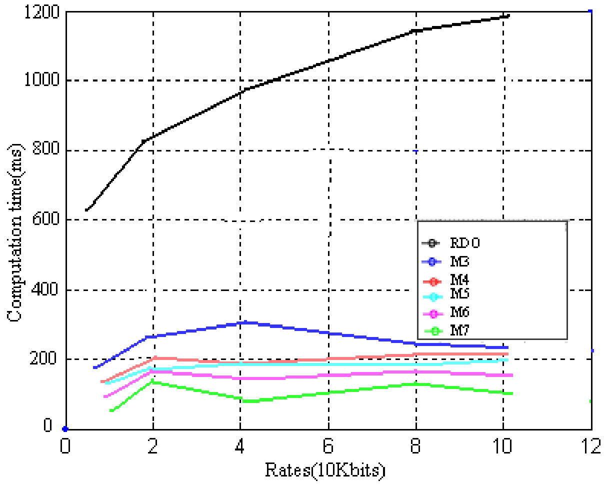

(b)

Figure 22: Stefan sequence, (IPPP seq.). (a) R-D performance, (b) computational complexity.

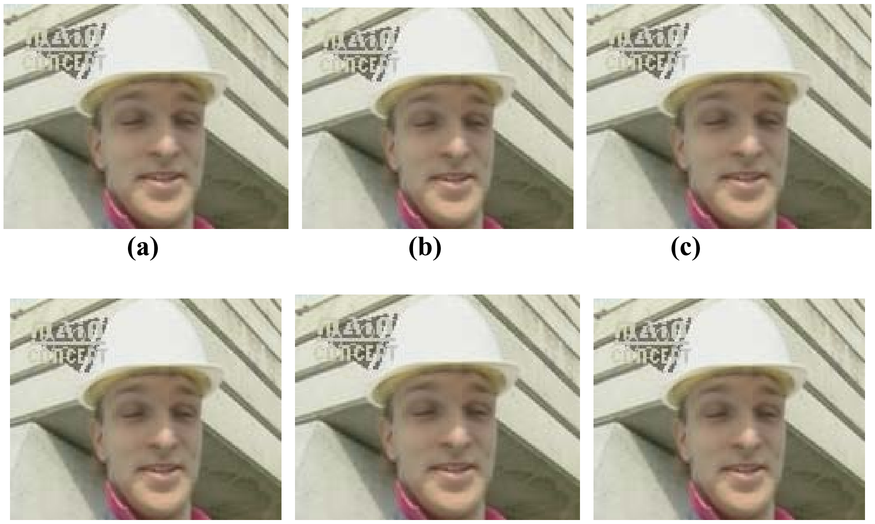

(a) **(b)** **(c)**

(d) **(e)** **(f)**

Figure 23: Quality of reconstructed frames of *Foreman* sequence: (a) RDO, (b) M3, (c) M4, (d) M5, (e) M6, (f) M7.

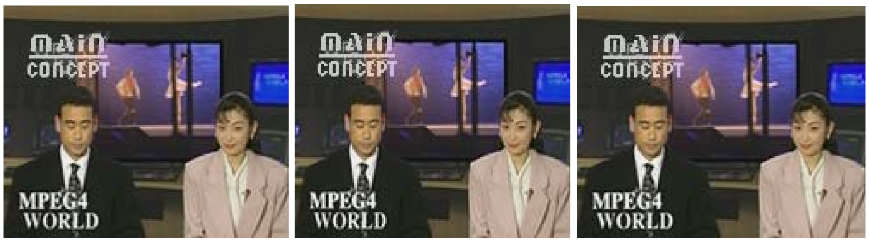

(a) **(b)** **(c)**

Figure 24: Quality of reconstructed frames of *News* sequence, (a) RDO, (b)M3, (c)M4, (d) M5, (e) M6, (f) M7.

References

[1] F. Pan, X. Lin, S. Rahardja, K. P. Lim, Z. G. Li, D. Wu, and S. Wu, "Fast Mode Decision Algorithm for Intra-prediction in H.264/AVC Video Coding", IEEE Trans. On circuits and systems for video Tech., Vol. 15, NO. 7, pp. 813-822, July 2005.

[2] T. Wiegand, G. J. Sullivan, G. Bjontegaard, and A. Luthra, "Overview of the H.264/AVC Video Coding Standard", IEEE Trans. On circuits and systems for video technology, Vol. 13, no. 13, no. 7, pp. 560-576, 2003.

[3] ece.ut.ac.ir/classpages/Multimedia/h264.ppt

[4] Envivio http://www.envivio.com/products/h264.html

[5] Changsung Kim, Qing Li, C. C. Jay Kuo, "Fast Intra-Prediction Model Selection for H.264 Codec," SPIE International Symposium ITCOM 2003, Orlando, Florida, Sept. 7-11, 2003.

[6] F. Pan, X. Lin, *et al.*, "Fast Mode Decision for Intra- Prediction," ISO/IEC JTC1/SC29/WG11 and ITU-T SG16 Q.6, JVT 7*th* Meeting, Pattaya II, Thailand, March 2003.

[7] F. Pan, X. Lin, S. Rahardja, K. P. Lim, and Z. G. Li, "A Directional Field Based Fast Intra-Mode Decision Algorithm for H.264 Video Coding," *IEEE Inter. Conf. on Multimedia and Expo*, vol. 2, pp. 1147-1150, June 2004.

[8] J. Kim and J. Jeong, "Fast Intra-Mode Decision in H.264 Video Coding Using Simple Directional Masks", Proc. of SPIE Vol. 5960, pp 1071-1079, 2005.

[9] R. Garg, M. Jindal, M. chauhan, "Statistics Based Fast Intra-Mode Detection", Proc. of SPIE Vol. 5960, pp 2085-2091, 2005.

[10] B. Jeon and J.lee, "Fast Mode Decision for H.264", ISO/IEC JTC1/SC29/WG11 and ITU-T SG16 Q.6, JVT 10th Meeting, Waikoloa, Hawaii, December 2003.

[11] C. Yang, L. PO, W. Lam, " A Fast H.264 Intra Prediction Algorithm Using Macroblock Properties", ICIP, pp. 461-464, 2004.

[12] B. Meng, O. C. AU, C. Wong, H. Lam, " Efficient Intra-Prediction Algorithm in H.264", IEEE, pp. 837-840, 2003.

[13] C. Tseng, H. Wang, J. Yang, " Improved and Fast Algorithms for Intra 4x4 Mode Decision in H.264/AVC", IEEE, pp. 2128-2131, 2004.

[14] C. Hsu, M. Ho, J. Hong, " An Efficient Algorithm for Intra-prediction in H.264", IEEE, pp. 35-36, 2006.

[15] Joint Video Team (JVT), reference software JM7.1, http://bs//hhi.de/~suehring/tml/download/JM7.1.zip.

[16] M. Jafari, S. Kasaei, " An Efficient Intra Prediction Mode Decision Algorithm for H.263 to H.264 Transcoding", IEEE international conference on computer systems and applications, page 1082-1089, march 2006.

[17] M. Jafari, s. Kasaei, " Prioritisation of data partitioned MPEG-4 video over GPRS/EGPRS mobile networks", Asian internet engineering conference (AINTEC), Tailand, pp. 68-82, December 2005.

[18] I. Richardson, " H.264/MPEG-4 part 10 white paper", available: http://www.vcodex.fsnet.co.uk/resources.html.

[19] C. Kim, H.-H. Shih, and C.-C. J. Kuo, "Feature-based intra-prediction mode decision for h.264," in *Proc. IEEE International Conference on Image Processing*, 2004.

[20] Chen Chen and Ping-Hao Wu, Hornor Chen," Transform-domain intra prediction for H.264", IEEE, pp. 1497-1500, 2005.

[21] G. Sullivan, "Recommended simulation common conditions for H.26L coding efficiency experiments on low resolution progressive scan source material," presented at the 14th VCEG-N81 Meeting, Santa Barbara, CA, Sep. 2001.

[22] Jiang Gang-yi, Li Shi-ping, Yu Mei, Li Fu-cui, " An efficient fast mode selection for intra prediction ", IEEE Int. Workshop VLSI Design & video Tech. , China, pp. 357-360, May 28-30, 2005.